UNIVERSIDAD NACIONAL DE COLOMBIA
SEDE MEDELLÍN
FACULTAD DE MINAS

DYNA
http://dyna.medellin.unal.edu.co/

Exergetic analysis of a dual-fuel engine, PEM electrolyzer and thermoelectric generator integrated system

Nelly De Armas-Calderón, Cristina Lizarazo-Bohórquez & Jorge Duarte-Forero

Facultad de Ingeniería, Universidad del Atlántico, Barranquilla, Colombia. ndearmas@est.uniatlántico.edu.co, cilizarazo@est.uniatlantico.edu.co, jorgeduarte@mail.uniatlantico.edu.co

Received: December 21th, 2019. Received in revised form: July 31th, 2020. Accepted: August 12th, 2020.

Abstract
In this research, the implementation of an integrated system composed of a dual-fuel engine (Diesel-Hydrogen), a PEM electrolyzer and a thermoelectric generator is envisioned. In order to know the optimal operating conditions of each sub-system, the exergetic efficiency and destroyed exergy were studied. It was estimated that for the dual combustion engine, the destroyed exergy would increase as a function of the concentration of methane in its mixture. By varying the electrical input to the electrolyzer, it was found that when the input current was 2A, the exergetic efficiency would go up to 92.59%, while for a current of 5A, the efficiency decreased in 51.80%. Finally, the exergetic efficiency of TEG decreased by increasing the hot flow temperature; 86.68% of the decrease in efficiency occurred for temperatures between 470K and 510K. On the other hand, the destroyed exergy increased linearly with an increase in the inlet temperature of exhaust gases.

Keywords: diesel engine; electrolyzer; exergetic analysis; hybrid systems; thermoelectric generator.

Análisis exergético de un sistema integrado de motor de combustible dual, electrolizador PEM y generador termoeléctrico

Resumen
En el presente artículo proyecta la implementación de un sistema integrado compuesto por un motor de combustión dual (Diesel-Hidrógeno), un electrolizador tipo PEM y un termogenerador eléctrico. En aras de conocer las condiciones óptimas de funcionamiento de cada subsistema se estudió la eficiencia exergética y la exergía destruída. Se estimó que para el motor combustión dual, la exergía destruída incrementa en función de la concentración de metano en su mezcla. Al variar la potencia eléctrica de entrada al electrolizador se encontró que cuando la corriente de entrada es de 2 A, su eficiencia exergética puede ser hasta 92.59 %, mientras que para una corriente de 5 A, la eficiencia disminuye un 51.80 %. Finalmente, la eficiencia exergética del TEG disminuyó con el aumento de la temperatura del flujo caliente, el 86.68 % del decrecimiento de eficiencia se dio en temperaturas entre 470 K a 510 K. En cambio, la exergía destruida incrementó linealmente al aumentar la temperatura de entrada de los gases de escape.

Palabras clave: análisis exergético; electrolizador; generador termoeléctrico; motor diesel; sistemas híbridos.

1. Introduction

Nowadays, the most important energy sources come from fossil resources [1] and their derivatives, such as oil, gas and primary energies, in order to obtain final energies. However, this practice is not sustainable due to population increase [2,3] and, consequently, to the high production and generation of energy that is required. According to the above, from the year 2000, the increase in ppm of CO_2 [4,5] as a result of excess energy consumed unnecessarily, has provided a significant increase in global pollution [6] and if this continues, by 2050, this will have increased the Earth's temperature to 2°C, at which point, changes are irreversible [7,8]. Consequently, strategies are proposed to ensure that

How to cite: Armas-Calderón, N, Lizarazo-Bohórquez, C. and Duarte-Forero, J, Exergetic analysis of a dual-fuel engine, PEM electrolyzer and thermoelectric generator integrated system. DYNA, 87(215), pp. 66-75, October - December, 2020.

this temperature increase does not exceed 0.5°C, which would be achieved by various means.

One of them comes from reforestation, which involves planting trees, as well as from generating electricity from nuclear energy [9] and renewable energy, thus leaving the possibility of significant change to the efficient use of energy.

For this reason, it is crucial to focus on the increase of renewable energies and their efficiency, for which it is common to use hybrid systems, as well as to study their thermodynamics. An answer to this would be thermoelectric generators (TEG), which can generate a voltage differential and thus obtain electric energy due to a temperature differential [10]. Because of its important applications, authors such as Murat et al. [11] have focused on thermodynamic studies that determine the energetic and exergetic efficiencies of each subsystem composing it. Similarly, Islam et al. [12] examined the operating conditions of a system, as well as its energy and exergetic influence on solar panels, such as in thermoelectric devices and concluded that the system presents a significant improvement by including thermoelectric generation.

On the other hand, hydrogen production using a proton-exchange membrane electrolyzer (PEM) provides a promising way to store and make better use of renewable energy resources. Nowadays, various studies on electrolyzers have focused on improving their energy and exergetic efficiencies to promote their technological progress. A. Kazim [13] performed an exergonomic analysis on a 12900 kW PEM electrolyzer, evaluating its performance under different operating temperatures and pressures; it was found that a 40% improvement in the exergetic cost of hydrogen can be achieved if the electrolyzer operates at low temperatures. However, a 2% decrease in the cost of exergy could be achieved if the operating pressure is increased from 1 to 10 atm. M. Leung et al. [14] developed energy and exergetic analyses to investigate the effect of the design, as well as the important operating parameters that account for the efficiency of a PEM electrolyzer plant. This study defined how much energy efficiency decreases with increasing operating temperature, decreasing current density, reducing electrolyte thickness and increasing electrode catalytic activity. In addition, F. Sorgulu & I. Dincer [15] studied a combined system consisting of a steam and gas turbine integrated with solar energy, to which they added an electrolyzer, to provide a sustainable energy resource based on hydrogen; through thermodynamic analysis, the different alternatives to increase the energy and exergetic efficiencies of the system were, in general, known. Moreover, with the help of studies related to exergetic efficiency, A. AlZahrani et al. [16] analyzed several operating conditions, state properties and the optimal production of hydrogen, using a model based on a solid oxide electrolyzer cell (SOEC).

As mentioned above, the increasing use of fossil fuels has caused serious problems for the environment [6]. Therefore, different countries have shown interest in making studies related to the environmental impact and emissions of fossil fuels, mainly those related to internal combustion engines. For this matter, the proposal of dual-fuel engines that use more environmentally friendly fuels was born; as a result, Da Costa et al. [17] evaluated, both theoretically and experimentally, the performance characteristics of an engine that operates dually using natural gas and diesel, performing energy and exergetic analyses and finding that both the energy and exergetic efficiencies increase when operated in this way. Moreover, other authors [18] have studied the performance of an engine operating only with alternative fuel, such as ethanol, in which the efficiencies of the first and second laws were evaluated as functions of engine speed, engine load and air-fuel ratio. O. Balli et al. [19] studied the effect of hydrogen fuel on the exergetic performance of a turbojet engine used in a military training aircraft, where the results indicated that the use of hydrogen seriously affects the exergetic performance of the engine and its components. However, the exhaust emissions to the environment decreased significantly.

Based on the above, the importance of integrating hybrid systems to achieve better overall performance is evident and thus, it is proposed to implement an integrated system consisting of a dual-fuel engine (diesel, hydrogen and air), a thermoelectric generator and an electrolyzer, which takes advantage of the high exhaust gas temperatures from the engine. Next, a thermoelectric generator obtains electric energy that is then used by a PEM electrolyzer to produce hydrogen that serves as a partial replacement of the engine's fuel. However, the work potential of this system is unknown, i.e., the maximum useful work that can be obtained from the system without violating thermodynamic laws, as well as the best performance that such systems can deliver [20]. In addition, in some cases, it is necessary to develop mathematical models that complement the thermal models to allow to predict the behavior of the analyzed systems [21,22]. Consequently, for future validation, the use of test stands is required since they are easy to use and provide extensive applications for research [23]. Therefore, this article aims to determine the optimal operating conditions of each subsystem by performing destroyed exergy and exergetic efficiency studies using thermodynamic models based on the second law, which is then compared with various references for support and validation. Once positive results have been obtained, the behavior of each subsystem in the references is analyzed by varying the parameters that influence their performance.

2. Methodology of thermodynamic modeling of each subsystem

According to the previous bibliographic references, the exergetic analyses have played a key role in the evaluation and improvement of the performance of a system, since by using them it is possible to identify the elements that exhibit higher irreversibility, to quantify them and to identify the sources that generate them [24]. In this regard, by studying the second thermodynamic law, opportunities are revealed to minimize the irreversibility and to maximize the global performance of any technical system, contrary to studying the first thermodynamic law, which only allows quantifying the

energy during a process and does not offer opportunities for improvement [25].

For this reason, this article is based on the principles of the second law of thermodynamics to obtain relevant information on the behavior of each sub-system, such as its exergetic efficiency and destroyed exergy and validating each model with bibliographic references.

2.1. System description

For this study, the basic functioning of three sub-systems was taken into account. In order to do the exergetic analysis of each system, it was necessary to take into account the mass and energy balances on the respective control volume.

Table 1 shows the measuring instruments used for each subsystem in order to know the variables involved.

Initially, a dual-fuel engine is considered that works at different powers. The description of the theoretical model is shown in Fig. 1, where the mass flow of diesel and methane is considered to enter the engine and mix with a mass flow of air; the mixture burns completely and the combustion products leave the engine. The engine produces an output power and transfers an amount of heat to the environment.

Table 1.
Instruments used for measurements

Engine			
Instrument	**Variable**	**Range**	**Accuracy**
Gas analyzer Ecom J2KN PRO	O_2	0 - 21 %v/v	±0.2 %
	CO	0 - 10000 ppm	±2 %
	NO	0 - 5000 ppm	±5 %
	NO_2	0 - 1000 ppm	±2 %
	SO_2	0 - 5000 ppm	±5 %
	H_2S	0 - 1000 ppm	±2 %
	CO_2	0 - 20 %v/v	±5 %
Power analyzer PCE-PA6000	Power	1W - 999.99kW	±1.5 %
Flow meter Fuel-View DFM-100	Diesel Flow	2 - 100 l/h	±1%
Flow meter FM-006RT-30	Gas flow	3-30 l/min	±4%
Electrolyzer			
Pressure Transmitter Model A-10	Pressure	0 to 1,000 bar	±0.5%
Temperature Sensor Pt 100 Type AA	Temperature	0 to 150°C	±0.1%*
Direct Read Variable Area Flow Meters FLDH3301C	Hydrogen Flow	Up to 1.5 L/min	±0.5%
Thermoeletric Generator			
Digital Display Voltmeter (Ammeter)	Volts Current	5 to 100 V 0.5 to 10A	±0.5%

*The industry standard accuracy at 0°C
Source: The Authors.

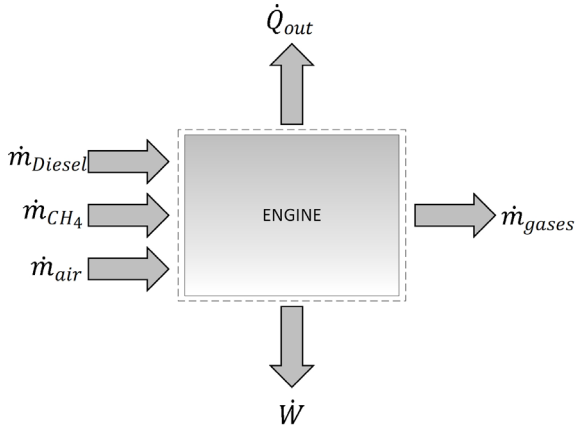

Figure 1. Schematic of the dual-fuel engine.
Source: The Authors.

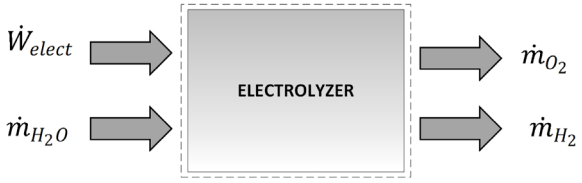

Figure 2. Schematic of the electrolyzer.
Source: The Authors.

Next, there is the theoretical model of a PEM electrolyzer, as shown in Fig. 2, having as inputs a constant electric current and a mass flow of water in the subcooled state, as well as output products that are decomposed by electrolysis, such as hydrogen and oxygen.

Finally, there is a thermoelectric generator that is a shell and tube heat exchanger with tubes covered with thermoelectric materials. The theoretical model of this subsystem, shown in Fig. 3, considers that the hot side is fed by the mass flow of hot flue gas coming from a turbine passing around the tubes, while the cold side is fed by seawater pumped by a circulating pump that flows inside the tubes. Since there is a temperature difference between both sides of the TEG, electricity is generated.

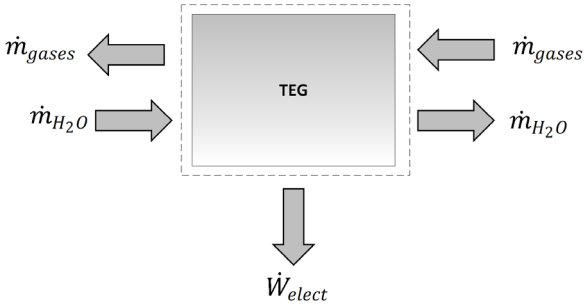

Figure 3. Schematic of the thermoelectric generator.
Source: The Authors.

The integrated system proposed by the authors aims to harness the potential energy from the exhaust gas stream of a dual-fuel engine, used as a hot fluid for a thermoelectric generator whose cold side is fed by water. This temperature differential will produce the electrical energy needed by an electrolyzer to obtain hydrogen that is then used as part of the fuel of the engine under dual operation. The studies mentioned above are intended to increase the overall efficiency of this system.

3. Thermodynamic model

The exergetic analysis applied to each sub-system was based on the second law of thermodynamics.

3.1. Exergetic analysis

For every sub-system, an exergetic analysis was performed by varying different input parameters, taking into account the following considerations:

- Every sub-system is in a stable state
- Sub-systems are treated as open systems and the reference state was defined as $T_0 = 293\ K$ and $P_0 = 1\ atm.$
- Exhaust gases were treated like air with an ideal behavior
- The mass flow of exhaust emissions from the engine is equal to the sum of the mass flow of diesel fuel, methane and air entering the combustion chamber
- The air entering in the combustion chamber is at ambient temperature and pressure, so it does not provide exergy to the sub-system
- The potential energy and kinetic effects of the flow of incoming and outgoing fluids are neglected
- Hydrogen and oxygen are treated as ideal gases
- In the electrolyzer, the exergy of water and oxygen is neglected

The exergy balance in a control volume can be generally expressed in terms of a ratio given by eq. (1):

$$\dot{X}_{in} - \dot{X}_{out} - \dot{X}_{destro} = \frac{dX_{syst}}{dt} \tag{1}$$

where the net energy transfer rate can be given by heat, work and mass, as expressed in eq. (2)-(4) :

$$X_{heat} = \dot{Q}\left(1 - \frac{T_0}{T}\right) \tag{2}$$

$$\dot{X}_{work} = \dot{W}_{útil} \tag{3}$$

$$\dot{X}_{mass} = \dot{m}\psi \tag{4}$$

The specific physical exergy was calculated according to Eq. (5):

$$\psi_{phy} = (h - h_0) - T_0(s - s_0) \tag{5}$$

For a compressed liquid, assuming the enthalpy h is given for low and moderate pressures and temperatures, it is possible to considerably reduce the error when evaluating h by:

$$h \cong h_{f@T} + v_{f@T}(P - P_{sat@T}) \tag{6}$$

Because hydrogen and oxygen were treated as ideal gases, their physical exergy is calculated by:

$$\psi_{phy(O)} = C_p T_0 \left[\frac{T}{T_0} - 1 - ln\left(\frac{T}{T_0}\right) + ln\left(\frac{P}{P_0}\right)^{(k-1)/k}\right] \tag{7}$$

The specific chemical exergy for diesel is given by Eq. (8):

$$\psi_{Die}^{chem} = H_u \cdot \varphi \tag{8}$$

where H_u is the net caloric value and φ is the chemical exergy factor, which, for liquid fuels, the effect of sulfur was included in the correlation according to the expression in [26]:

$$\varphi = 1.0401 + 0{,}1728 \cdot \frac{h}{c} + 0{,}0432 \cdot \frac{o}{c} + 0.2169 \cdot \frac{\propto}{c}\left(1 - 2.0628 \cdot \frac{h}{c}\right) \tag{9}$$

where h, c, o and $\propto$ are the mass fractions of H, C, O and S, respectively. The accuracy of this expression is estimated to be ±0.38%.

The efficiency of the second law for each subsystem is shown in Table 2.

3.2. Validation

According to the previous studies related to the second thermodynamic law behavior of dual combustion engines, the thermoelectric generators and electrolyzers allow comparison and validation between the models proposed by each author and those presented in this article. Therefore, what has been proposed is validated.

Table 2.
Exergetic efficiency for each sub-system.

Sub-System	Exergetic efficiency
Engine	$\eta_{II} = \frac{\dot{W}}{X_{Diesel} + X_{CH_4}}$ (10)
Electrolyzer	$\eta_{II} = \frac{X_{H_2} + X_O - X_{H_2O}}{\dot{W}_{elect}}$ (11)
Thermoelectric generator	$\eta_{II} = \frac{\dot{m}_{seawater}(\psi_{in} - \psi_{out}) + \dot{W}_{electric}}{\dot{m}_{gases}(\psi_{in} - \psi_{out})}$ (12)

Source: The Authors.

3.2.1. Dual combustion engine

Ramos da Costa et al. [17] studied an electro-mechanical system composed of a commercial engine (Cummins 6CTA) with mechanical power of 188kW at 1800 rpm, equipped with air, gas and diesel flow meters, temperature and pressure sensors at different points making it ideal for gas analysis. For this, it is assumed that the air enters at standard conditions and therefore does not contribute exergy to the system. Similarly, fuels (diesel and natural gas) enter at ambient pressure and temperature, so the exergy provided by these amounts only to specific chemical exergy. The data in Table 3, provided by the author, is considered.

Costa et al. [17] varied the engine power in a range between 10 kW and 150 kW, with increments of 10 kW and different mass flows of diesel fuel and methane for each variation.

Fig. 4 shows the behavior of the exergetic efficiency as a function of the engine power, where it is evident that for higher power values, the second law efficiency improved significantly. When increasing the load from 80 kW to 150 kW, this efficiency increased by 55.55% until reaching its maximum value; this is due to greater use of the exergy contributed by the fuels. The highest error calculated was 28.775% with respect to the data revealed by the study of the previous author, as shown in Table 4.

As the load on the engine increased, the total exergy input increased, as shown in Fig. 5. From 80 kW to 150 kW, the total exergy input increased by 17.04%. The calculated data revealed a maximum error of 16.1% compared to the data provided by Costa et al. [17], as shown in Table 5.

Moreover, they calculated the exergy destroyed for different powers. This resulted in Fig. 6, where it is observed that the exergy is approximately constant, i.e., the exergy shows few variations when altering power-which is congruent with the results in this article-and reveals a maximum power error of 31.217%, as shown in Table 6.

Table 3.
Experimental data of the engine.

Power [kW]	Mass Flow rate of diesel (kg/h)	Mass Flow rate of air (kg/h)	Mass Flow rate of gas (kg/h)
11.7	6.53	717.480	8.590
19.2	7.91	755.930	9.420
29.3	10.17	800.400	10.010
40.0	11.92	852.900	10.570
48.1	14.52	903.340	11.330
58	15.32	947.190	11.810
68.2	17.22	1010.130	12.550
77.2	19.73	1065.950	13.140
86.7	22.29	1119.190	14.010
93.4	24.16	1197.840	14.400
103.3	25.44	1265.140	14.970
111.1	26.97	1311.310	15.850
122.9	27.29	1369.330	16.150
132.5	31.17	1440.290	16.590
140 .3	32.43	1491.850	14.340

Source: Adapted from Costa et al. [17].

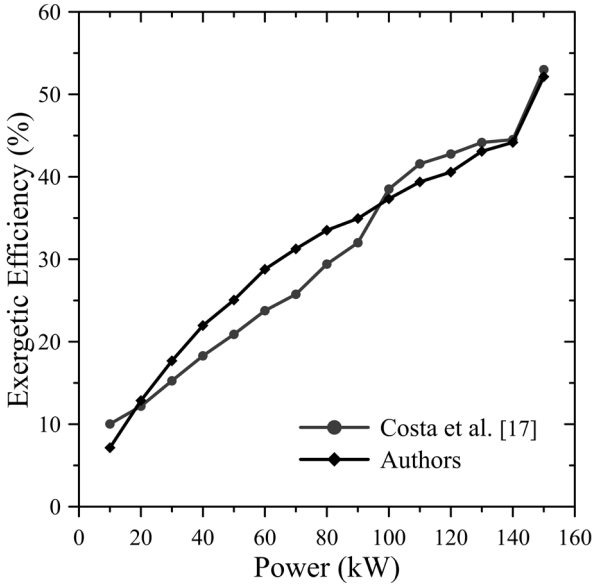

Figure 4. Exergetic efficiency as a function of power.
Source: The Authors.

Table 4.
Exergetic efficiency as a function of power.

Potencia [kW]	Exergetic Efficiency		
	Costa et al. [17]	Authors	Error (%)
11.7	10.020	7.137	28.775
19.2	12.180	12.859	5.577
29.3	15.259	17.681	15.867
40.0	18.289	21.963	20.09
48.1	20.887	25.054	19.95
58.0	23.758	28.779	21.134
68.2	25.750	31.264	21.417
77.2	29.407	33.519	13.983
86.7	32.001	34.937	9.177
93.4	38.509	37.328	3.067
103.3	41.570	39.383	5.26
111.1	42.757	40.566	5.125
122.9	44.157	43.091	2.413
132.5	44.514	44.168	0.775
140 .3	53.000	52.14	1.623

Source: The Authors.

Table 5.
Total exergy as a function of power.

Power [kW]	Total Exergy (kW)		
	Costa et al. [17]	Authors	Error (%)
11.7	141.636	140.120	1.083
19.2	151.277	155.529	2.734
29.3	159.09	169.678	6.240
40.0	169.919	182.120	6.700
48.1	178.004	199.569	10.806
58.0	188.653	208.485	9.512
68.2	202.276	223.897	9.656
77.2	211.901	238.67	11.216
86.7	225.450	257.603	12.482
93.4	228.085	267.895	14.861
103.3	234.354	279.308	16.095
111.1	248.374	295.813	16.037
122.9	266.310	301.686	11.726
132.5	293.390	265.226	10.619

Source: The Authors.

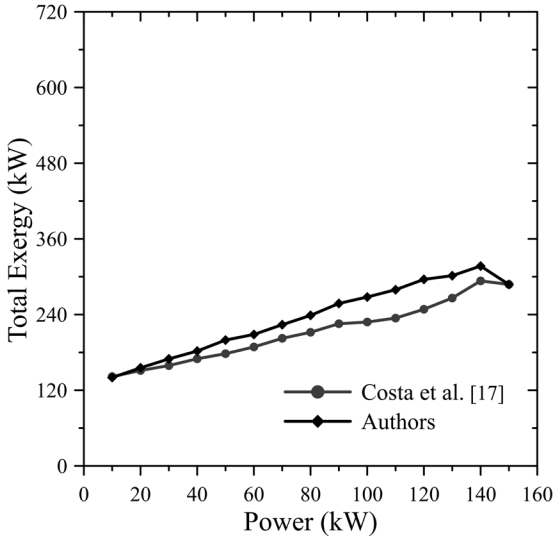

Figure 5. Total exergy as a function of power.
Source: The Authors.

Table 6.
Exergy destroyed as a function of power.

Potencia	Exergy destroyed (kW)		
[kW]	Costa et al.	Authors	Error (%)
11.7	100.55	95.414	5.108
19.2	102.50	98.957	3.456
29.3	101.60	101.197	0.397
40.0	101.75	101.318	0.425
48.1	101.30	106.49	5.123
58.0	99.950	103.676	3.728
68.2	100.250	106.294	6.029
77.2	99.650	108.649	9.030
86.7	100.10	115.097	14.982
93.4	98.15	112.089	14.202
103.3	96.80	110.552	14.207
111.1	98.45	114.843	16.651
122.9	99.80	108.131	8.348
132.5	103.85	109.877	5.804

Source: The Authors.

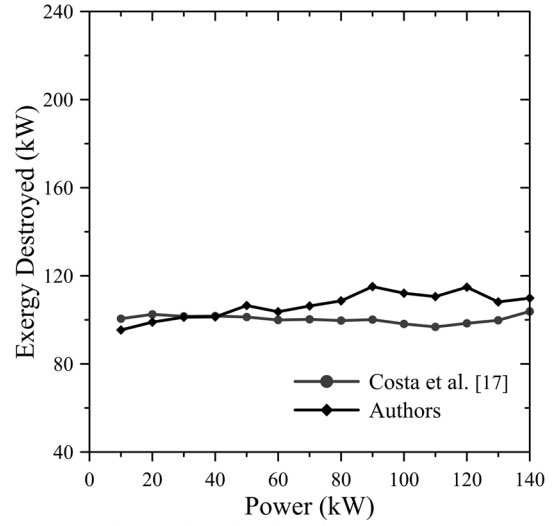

Figure 6. Exergy destroyed as a function of power.
Source: The Authors.

3.2.2. Electrolyzer

In order to validate the electrolyzer, the results obtained by Caliskan et al. [27] were taken as a reference, in which an exergetic analysis was developed for a PEM electrolyzer with 10 cells. The parameters used in the case studies are shown in Table 7.

Table 7.
Parameters of the electrolyzer

Parameter	Value
Voltage	11.32 V
Current	3.8 A
Maximum pressure	6 bar
Working temperature	15ºC - 45ºC
Temperature of hydrogen	28ºC
Hydrogen pressure	1.05 bar
Specific heat capacity of hydrogen	14.309 kJ/kg K
Volumetric flow rate of hydrogen	$2.4\ x\ 10^{-6}$ m^3/s
Mass flow of hydrogen	$1.91\ x\ 10^{-7}$ kg/s
Density of hydrogen	0.07998 kg/m^3
Adiabatic exponent	1.4
Standard chemical exergy of hydrogen	118298.61 kJ/kg
Environment temperature	30ºC
Environment pressure	1 bar

Source: Adapted from Caliskan et al. [27].

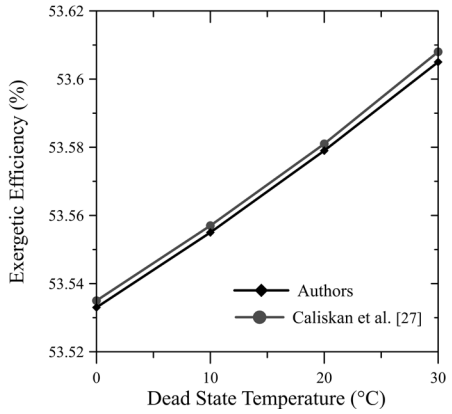

Figure 7. Exergy efficiency as a function of the dead state temperature.
Source: The Authors.

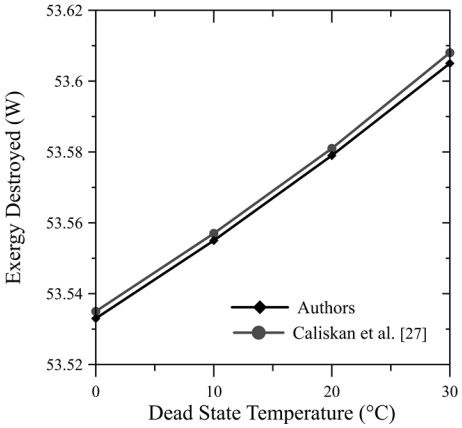

Figure 8. Exergy destruction as a function of the dead state temperature.
Source: The Authors.

Table 8.
Comparison of values obtained for the exergy efficiency.

	Dead State Temperature °C			
	0	**10**	**20**	**30**
Caliskan et al. (%)	53.535	53.557	53.581	53.608
Authors (%)	53.533	53.555	53.579	53.605
Error (%)	0.004	0.004	0.0004	0.004

Source: The Authors.

Table 9.
Comparison of values obtained for the exergy destruction.

	Dead State Temperature °C			
	0	**10**	**20**	**30**
Caliskan et al.	19.987 kW	19.978 kW	19.967 kW	19.956 kW
Authors	19.988 kW	19.979 kW	19.968 kW	19.957 kW
Error (%)	0.005	0.005	0.0005	0.005

Source: The Authors.

Using Figs. 7 and 8, it was observed that the results of the reference model show congruence with those proposed in this article, with an error of 0.004% and 0.005%, respectively. Tables 8 and 9 show the results obtained in this article and those in the reference.

3.2.3. Thermoelectric generator

In order to validate correctly the exergetic analysis performed on this subsystem, the results of Demir et al. [28] were taken into account, where an exergetic analysis of a hybrid cogeneration system for electricity and freshwater production was performed. The system consists of a solar-natural gas hybrid power plant, a thermoelectric generator (TEG), a Rankine cycle to produce electricity and a flash distillation unit to produce fresh water. The TEG unit is used to take advantage of the gases produced by the gas turbine, where tin sulfide (SnS) and bismuth telluride (Be_2Te_3) is the selected thermoelectric materials for the TEG. The parameters considered were 100kPa, 25°C for the atmospheric conditions and a gas turbine flow rate of 42.26 kg/s. The hot side of the TEG is fed by flue gases at 227°C and 100 kPa, which then leaves the TEG at 189°C and the same inlet pressure. In addition, the cold side of the TEG is fed by seawater pumped by a circulating pump at 20°C and exits the TEG under slightly different conditions. For that reason, the exergy of the cold side of the TEG is neglected.

According to the parameters above, the destroyed exergy and the efficiency were calculated and plotted in Fig. 9.

By comparing the results of the models, it follows that, as shown in Table 10, the error rate for both study cases is approximately 2% and thus, it is within the allowed range.

Table 10.
Comparison of values obtained for the exergy destruction and exergy efficiency

	Exergy Destruction (kW)	**Exergy Efficiency (%)**
Demir et al. [28]	585.8	5.32
Authors	596.52	5.23
Error	0.018	0.016

Source: The Authors.

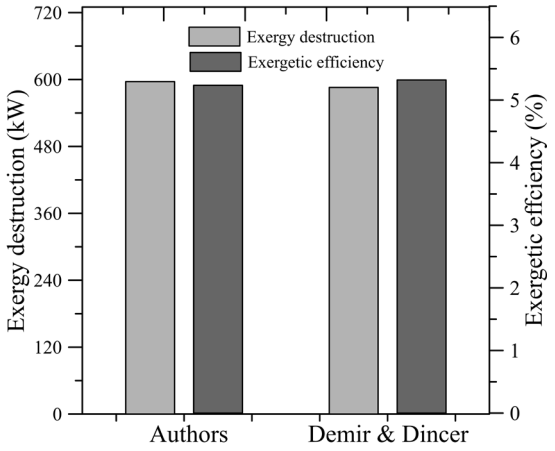

Figure 9. Exergy destruction and exergy efficiency by Demir et al. and authors.
Source: The Authors

In both cases, it is possible to show that the behavior is congruent since by obtaining higher exergy destroyed using the model proposed in this article, it was expected that the exergetic efficiency was lower than that of Demir et al.

4. Results and discussion

For each sub-system, a case study was applied by varying different parameters and analyzing the results obtained.

4.1. Case study I: Dual-fuel engine

In the dual-fuel engine, the behavior of the exergy destroyed and the exergetic efficiency as a function of methane concentrations for three different power values was analyzed using their respective fuel mass flows. Initial concentrations were 10% methane and 90% diesel, increasing the concentration of methane by 10 percent. This resulted in Fig. 10, where it was observed that the exergy destroyed is directly proportional to the concentration of methane; moreover, it can be inferred that more exergy is destroyed when the power or the slope is increased, i.e., at higher power levels, the sensitivity to destroy exergy is greater with increasing methane concentrations.

For the lower power level, for every 10% increase in methane concentrations, the exergy destroyed increases by 18.016 W. For the medium power, it increases by 39.166 W and for the highest power, the exergy destroyed increases by 55.728 W.

On the other hand, the exergetic efficiency decreases whenever the mixture contains higher levels of methane; however, for higher power levels, the exergetic efficiency increased. For the studied interval of CH_4 concentrations, the exergetic efficiency decreased by 72.10% for 11.7 kW, varying from 5.85% to 20.97%; for 77.2 kW, the exergetic efficiency decreased by 63.08%, varying from 17.76% to 48.12% and, for 140.3 kW, the exergetic efficiency decreased by 63.08%, varying from 22.69% to 61.46%.

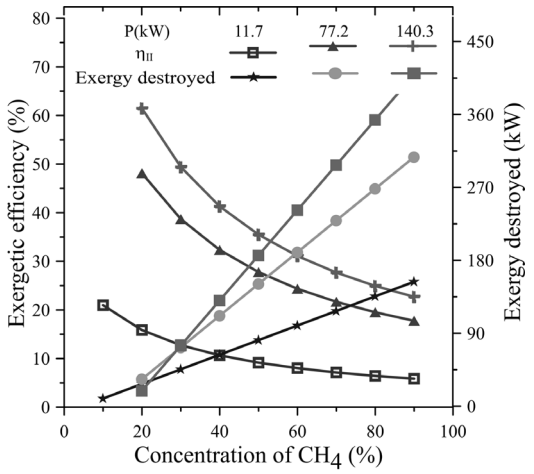

Figure 10. Exergetic efficiency and Exergy destroyed as a function of the concentration of CH_4.
Source: The Authors.

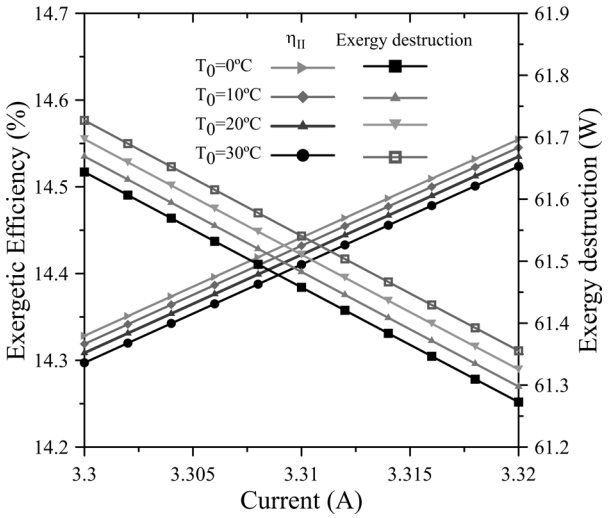

Figure 12. Exergetic efficiency and Exergy destruction as a function of a shorter current interval.
Source: The Authors.

4.2. Case study II: Electrolyzer

The input exergy was modified in the electrolyzer by modifying the input current from 2.2A to 5A in increments of 0.4A and keeping the voltage constant at four different reference temperatures.

The results are shown in Fig. 11, where it is observed, on a macroscopic scale, how the exergetic efficiency potentially decreases for every change in current levels. Thus, for 2.2 A, the efficiency reached a maximum of 92.5915% and, for 5A, the efficiency decreased by 51.8%, reaching 40.74%. This happens because by supplying a higher current during the electrolysis process, the input exergy to the electrolyzer increases, whereas by keeping the output exergy constant, the exergetic efficiency will be lower; this is consistent with the research done by Esmaili et al. [29], as well as Meng Ni et al. [14].

Moreover, the exergy destroyed increased linearly as a function of the current; this means that for every 0.4 amperes of input current, the exergy destroyed increased by 4.53 watts.

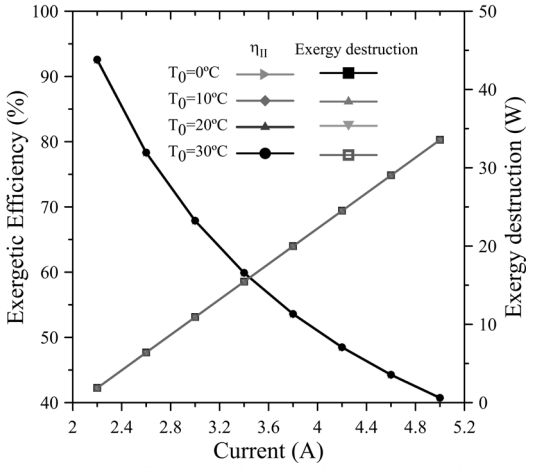

Figure 11. Exergetic efficiency and Exergy destruction as a function of the current.
Source: The Authors.

Meanwhile, for every 10°C decrease in the dead state temperature, the destroyed exergy increased by approximately 0.1%. In addition, the above-mentioned authors also agree with an increase of the irreversibilities at greater current levels. This is due to the activation overpotential of the anode, cathode, as well as the electrolyte's ohmic overpotential. The ohmic overpotential close to the proton-exchange membrane is related to the resistance of the membrane to hydrogen ions crossing it. The ionic resistance is a function of humidification, thickness and temperature of the proton-exchange membrane. In addition, the activation overpotential corresponds to the energy barrier that has to be overcome in order to start a redox electrochemical reaction, especially those related to the electron transfer that happens at the electrode interface [30].

Fig. 12 shows the behavior of the exergetic efficiency and exergy destruction for a shorter input current interval. This allows to observe the changes whenever the reference temperature is modified, for this is done on a smaller scale.

4.3. Case study III: Thermoelectric Generator (TEG)

In the TEG, the behavior of the exergetic efficiency and the exergy destroyed was analyzed by varying the flue gas inlet temperature from 470 K to 560 K in 10 K increments, for mass flows of 32.26 kg/s, 42.36 kg/s and 52.36 kg/s. The results of this analysis are shown in Fig. 13, where the behavior of the exergetic efficiency as a function of the different exhaust gas temperatures, as well as the destroyed exergy, is observed.

For the three mass flows analyzed, 86.68% of the decrease in the exergetic efficiency occurred between 470 K and 510 K; this means that from 510 K, the exergetic efficiency values showed minimal variation.

Moreover, the destroyed exergy displayed a linear behavior for changes in flue gas temperature. An increase in the mass flow of flue gases also produced an increase in the

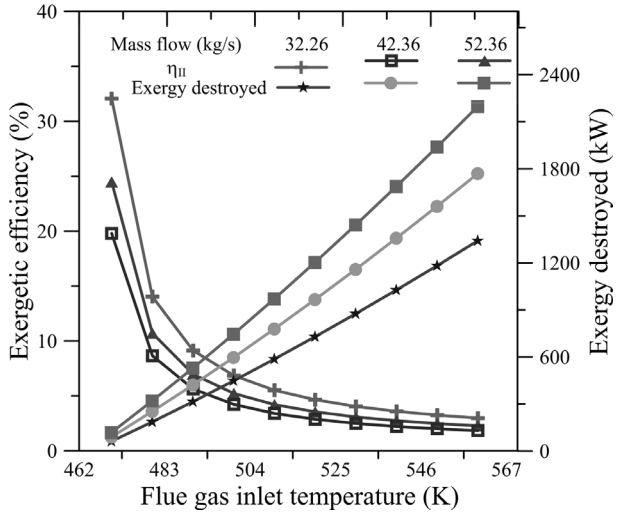

Figure 13. The variation of the exergetic efficiency and the exergy destroyed by changing the flue gas inlet temperature.
Source: The Authors

destroyed exergy. For the lowest temperature analyzed, this resulted in increases of 45.63% and 31.33% for every variation in the mass flow, while for the maximum temperature analyzed, the increase was 31.95% and 24.21%, respectively.

5. Conclusion

The exergetic analysis is a fundamental tool at the time of evaluating the performance of a system, as it allows to quantify the irreversibilities of a process, make comparisons and identify opportunities for improvement. Therefore, it is very useful to apply these analyses to hybrid systems when it comes to evaluating their thermodynamic behavior. In order to know the useful work and the efficiency that the system proposed in this article would have (dual-fuel engine - TEG - electrolyzer), it was necessary to do this type of analysis where the exergetic models of each subsystem were compared and their reliability was determined through validation using different references, resulting in average errors of around 10% for the engine, less than 0.01% for the thermoelectric generator and less than 0.02% for the recuperator. It was also observed that for a dual fuel engine (diesel and natural gas), varying the concentration of methane from 10% to 90%, for the power of 11.7 kW, caused a decrease in the exergetic efficiency of 72.10%, whereas, for 77.2 kW and 140.3 kW, this resulted in a decrease by 63.08% in both cases. In addition, for every 10% increase in methane concentrations, the destroyed exergy increased by 18.02 kW for 11.7 kW, 37.17 kW for 77.2 kW and 55.73kW for an operating power of 140.3kW. The latter results also show that the exergy destroyed is greater when the operating power of the engine increases.

In the case of the electrolyzer, it was observed that an increase in the input current significantly affected the exergetic efficiency of the electrolyzer: as the input current varied from 2.2A to 5A, for reference temperatures of 0ºC, 10ºC, 20ºC and 30ºC, the exergetic efficiency decreased by 56% in all cases. The latter is to be compared with the destroyed exergy, which increased notably by 94.41%, 94.44%, 94.47% and 94.50%, respectively, as a result of the variation of the above-mentioned parameters. On the other hand, for the TEG, it was noticed that the exergetic efficiency decreased whenever there was an increase in the flue gas inlet temperature; the most significant changes occurred from 470 K to 510 K, as this amounted to 86.68% of the total decrease. Furthermore, the destroyed exergy increased linearly by increasing the flue gas inlet temperature, as well as by modifying the mass flow of the fluid. For mass flows of 32.26 kg/s, 42.36 kg/s and 52.36 kg/s, the exergy destroyed ranged from 61.64kW to 1382.10kW, 89.77kW to 1769.29kW and 117.90kW to 2197.71kW, respectively.

This study gives a clear idea of the optimal operating conditions of the studied sub-systems. In future works, it is intended to integrate them and to reach high global performance.

6. Nomenclature

Symbol	Name	Unit
X_{in}	Exergy input	kW
X_{out}	Exergy output	kW
X_{destro}	Exergy destroyed	kW
ΔX_{syst}	Change of exergy in the system	kW
X_{H_2}	Hydrogen exergy	kW
X_O	Oxygen exergy	kW
X_{H_2O}	Water exergy	kW
X_{Diesel}	Diesel exergy	kW
X_{heat}	Exergy transferred to the environment	kW
X_{CH_4}	Methane exergy	kW
ψ	Specific exergy of flow	kJ/kg
$\dot{Q}_{out}$	The waste heat by the engine to the environment	kW
$\dot{W}$	Power of engine	kW
$\dot{W}_{elect}$	Electrical exergy input	kW
$\dot{m}_{Diesel}$	Mass flow rate of water diesel	kg/s
$\dot{m}_{CH_4}$	Mass flow rate of water methane	kg/s
$\dot{m}_{air}$	Mass Flow rate of air	kg/s
$\dot{m}_{exhaust}$	Mass flow rate of exhaust gases	kg/s
$\dot{m}_{H_2O}$	Mass flow rate of water	kg/s
$\dot{m}_{H_2}$	Mass flow rate of hydrogen	kg/s
$\dot{m}_O$	Mass flow rate of oxygen	kg/s
$T_{out,exhaust}$	Exhaust gases outlet temperature	K
T_0	Standard temperature	K
T_f	Temperature of the system boundary where heat ist ransferred t o the environment	K
η_{II}	Exergetic efficiency	%

References

[1] Gautam, P., Kumar, S. and Lokhandwala, S., Energy-Aware Intelligence in Megacities. Chapter 11, Elsevier B.V., 2019. DOI: 10.1016/B978-0-444-64083-3.00011-7

[2] Preston, S.H. The effect of population growth on environmental quality, Population Research and Policy Review, 15(2), pp. 95-108, 1996. DOI: 10.1007/BF00126129.

[3] Shi, A., The impact of population pressure on global carbon dioxide emissions, 1975-1996: evidence from pooled cross-country data., Ecological Economics, 44(1), pp. 29-42, 2003. DOI: 10.1016/S0921-8009(02)00223-9.

[4] Brovkin, V., Sitch, S., Von Bloh, W., Claussen, M., Bauer, E. and Cramer, W., Role of land cover changes for atmospheric CO_2 increase and climate change during the last 150 years. Global Change Biology 10(8), pp. 1253-1266, 2004. DOI: 10.1111/j.1365-2486.2004.00812.x.

[5] Kurihara, H. and Shirayama, Y., Effects of increased atmospheric CO_2 on sea urchin early development, 274, pp. 161-169, 2004. DOI: 10.3354/meps274161.

[6] Bilgen, S., Structure and environmental impact of global energy consumption. Renewable and Sustainable Energy Reviews, 38, pp. 890-902, 2014. DOI: 10.1016/j.rser.2014.07.004.

[7] Hansen, J., Ruedy, R., Sato, M. and Lo, K., Global surface temperature change. Reviews of Geophysics, 48(4), 2010. DOI: 10.1029/2010RG000345

[8] New, M., Liverman, D., Schroder, H. and Anderson, K., Four degrees and beyond: the potential for a global temperature increase of four degrees and its implications, 2011. DOI: 10.1098/rsta.2010.0303.

[9] Revankar, S.T., Nuclear Hydrogen Production. Elsevier Inc., 2019. DOI: 10.1016/B978-0-12-813975-2.00004-1.

[10] Champier, D., Thermoelectric generators: a review of applications. Energy Conversion and Management, 140, pp. 167-181, 2017. DOI: 10.1016/j.enconman.2017.02.070.

[11] Demir, M.E. and Dincer, I., Development of a hybrid solar thermal system with TEG and PEM electrolyzer for hydrogen and power production. International Journal of Hydrogen Energy, 42(51), pp. 30044-30056, 2017. DOI: 10.1016/j.ijhydene.2017.09.001.

[12] Islam, S., Dincer, I. and Yilbas, B.S., Energetic and exergetic performance analyses of a solar energy-based integrated system for multigeneration including thermoelectric generators. Energy, 93, pp. 1246-1258, 2015. DOI: 10.1016/j.energy.2015.09.111.

[13] Kazim, A.M., Exergoeconomic analysis of a PEM electrolyser at various operating temperatures and pressures. International Journal of Energy Research, 29(6), pp. 539-548, 2005. DOI: 10.1002/er.1073.

[14] Ni, M., Leung, M.K. and Leung, D.Y., Energy and exergy analysis of hydrogen production by a proton exchange membrane (PEM) electrolyzer plant. Energy Conversion and Management, 49(10), pp. 2748-2756, 2008. DOI: 10.1016/j.enconman.2008.03.018.

[15] Sorgulu, F. and Dincer, I., Thermodynamic analyses of a solar-based combined cycle integrated with electrolyzer for hydrogen production. International Journal of Hydrogen Energy, 43(2), pp. 1047-1059, 2018. DOI: 10.1016/j.ijhydene.2017.09.126.

[16] Al Zahrani, A.A. and Dincer, I., Thermodynamic and electrochemical analyses of a solid oxide electrolyzer for hydrogen production. International Journal of Hydrogen Energy, 42(33), pp. 21404-21413, 2017. DOI: 10.1016/j.ijhydene.2017.03.186.

[17] da Costa, Y.J.R., de Lima, A.G.B., Bezerra Filho, C.R. and de Araujo-Lima, L., Energetic and exergetic analyses of a dual-fuel diesel engine. Renewable and Sustainable Energy Reviews, 16(7), pp. 4651-4660, 2012. DOI: 10.1016/j.rser.2012.04.013.

[18] Rufino, C.H., de Lima, A.J., Mattos, A.P., Allah, F.U., Bernal, J.L., Ferreira, J.V. and Gallo, W.L.Exergetic analysis of a spark-ignition engine fuelled with ethanol. Energy Conversion and Management, 192, pp. 20-29, 2019. DOI: 10.1016/j.enconman.2019.04.035.

[19] Balli, O., Sohret, Y. and Karakoc, H.T., The effects of hydrogen fuel usage on the exergetic performance of a turbojet engine. International Journal of Hydrogen Energy, 43(23), pp. 10848-10858, 2018. DOI: 10.1016/j.ijhydene.2017.12.178.

[20] Amador-Diaz, G., Duarte-Forero, J., Garcia, J., Rincon, A., Fontalvo, A., Bula, A. and Vazquez-Padilla, R., Maximum power from fluid flow by applying the first and second laws of thermodynamics. Journal of Energy Resources Technology. ASME, 139(3)pp. 1-8, 2017. DOI: 10.1115/1.4035021.

[21] Duarte-Forero, J.E., Estrada, W.G. y Guerrero, J.S., Desarrollo de una metodología para la predicción del volumen real en la cámara de combustión de motores diésel utilizando elementos finitos. Inge Cuc, 14(1), pp. 122-132, 2018. DOI: 10.17981/ingecuc.14.1.2018.11.

[22] Consuegra, F., Bula, A., Guillín, W., Sánchez, J. and Duarte-Forero, J.E., Instantaneous in-cylinder volume considering deformation and clearance due to lubricating film in reciprocating internal combustion engines. Energies, 12 (8), 2019. DOI: 10.3390/en12081437.

[23] Narvaez-Pallares, H., Villareal-Acosta, S., Duarte-Forero, J.E. and Rincon-Montenegro, A., Implementación de un banco para pruebas en motor Diésel monocilíndrico con aplicaciones investigativas. Scientia et technica, 22(4), pp. 330-340, 2017. DOI: 10.22517/23447214.16111.

[24] Bejan, A., Tsatsaronis, G. and Moran, M.J., Thermal Design and Optimization, John Wiley, USA, 1995.

[25] Cengel, Y.A. and Boles, M., Termodinámica-Cengel 7th Ed., McGrow Hill, México, 2011.

[26] Kotas, T.J., Appendix C Chemical exergy of industrial fuels, in: The Exergy Method of Thermal Plant Analysis, 1985, pp. 267-269. DOI: 10.1016/C2013-0-00894-8.

[27] Caliskan, H., Dincer, I. and Hepbasli, A., Energy, exergy and sustainability analyses of hybrid renewable energy based hydrogen and electricity production and storage systems: modeling and case study. Applied Thermal Engineering, 61(2), pp. 784-798, 2013. DOI: 10.1016/j.applthermaleng.2012.04.026.

[28] Demir, M.E. and Dincer, I., Development of an integrated hybrid solar thermal power system with thermoelectric generator for desalination and power production. Desalination, 404, pp. 59-71, 2017. DOI: 10.1016/j.desal.2016.10.016.

[29] Esmaili, P., Dincer, I. and Naterer, G.F., Energy and exergy analyses of electrolytic hydrogen production with molybdenum-oxo catalysts. International Journal of Hydrogen Energy. International Journal of Hydrogen Energy, 37(9), pp. 7365-7372, 2012. DOI: 10.1016/j.ijhydene.2012.01.076.

[30] Carmo, M., Fritz, D.L., Mergel, J. and Stolten, D., A comprehensive review on PEM water electrolysis. International Journal of Hydrogen Energy, 8(1), pp. 4901-4934, 2013. DOI: 10.1016/j.ijhydene.2013.01.151.

N.A. De Armas-Calderón, born in Barranquilla-Colombia. Is student Eng. in Mechanical and Industrial Engineer fro the Universidad del Atlántico, Colombia.
ORCID: 0000-0002-1640-5921

C.I. Lizarazo-Bohórquez, born in Barranquilla-Colombia. Is student Eng. In Mechanical Engineer student at Universidad del Atlántico, Colombia.
ORCID: https://orcid.org/0000-0001-8387-0359

J. Duarte-Forero, born in Barranquilla, Colombia. He is an associated professor of the Mechanical Engineering Program from the Universidad del Atlántico. He received his BSc. Eng. in Mechanical Engineering in 2007 from the Universidad del Atlántico, Barranquilla, Colombia. MSc. in Mechanical Engineering in 2013, from the Universidad del Norte, Barranquilla, Colombia. PhD. in Engineering in 2017, from the Universidad del Norte, Colombia. He is a COLCIENCIAS - Senior Researcher.
ORCID: 0000-0001-7345-9590